

Numerical investigation of deposition mechanism of submarine debris flow

Dingzhu Liu^{a,b,*}, Yifei Cui^{c*}, Clarence E. Choi^{c,d}, Nazir Ahmed Bazai^{a,b}, Zhilin Yu^e,
Mingyu Lei^{a,b}, Yanzhou Yin^{a,b}

^aKey Laboratory of Mountain Hazards and Earth Surface Process, Institute of Mountain Hazards and Environment, Chinese Academy of Sciences, Chengdu 610041, China

^bUniversity of Chinese Academy of Sciences, Beijing 100049, China

^cDepartment of Civil and Environmental Engineering, Hong Kong University of Science and Technology, Clear Water Bay, Hong Kong, China

^dThe HKUST Jockey Club Institute for Advanced Study, HKSAR, Hong Kong, China

^eSouthwest Electric Power Design Institute, Chengdu 610021, China

Abstract

Submarine debris flow can damage oil and gas transport pipelines with potentially adverse consequences to the environment and to the industrial activity itself. The deposition process of submarine debris flow, which is related to the flow viscosity, is complex due to the slurry diffusion process that happens during the interaction of water and slurry. In addition, a quantitative characterization of the characterize the flow mechanism as influenced by the material density during the deposition process remains a scientific challenge. To fundamentally understand the mechanisms of solid-fluid interactions in fast-flowing submarine debris flows, a series of three-dimensional (3D) numerical simulations using Computational Fluid Dynamics (CFD) were conducted. The Herschel-Bulkley (HB) model was used to define the submarine slurry's rheological characterization as calibrate through simple rheological experiment. Results reveal that deposition is a mass diffusion process. Shear stress at the bottom and at the top of the slurry leads to velocity differences in the vertical direction which in turn generates a huge vortex, which contributed to a separation of slurry into two parts: the frontal head, and the tail. The velocity difference in vertical direction is helpful for hydroplaning. For higher slurry viscosity case, the flow profile is longer and thicker with a front head that has a lower averaged densities and sharper head angles. In addition, highly viscous slurries have lower average frontal velocities during the deposition process. The mixture density decreases in two stages: quick decreasing stage and stable decreasing stage. In the first stage, the slurry expands quicker than the second stage. Higher viscosities also lead to larger volume expansions which consequently leads to quicker density decrease.

Keywords: Submarine debris flow; Deposition mechanism; Computational fluid dynamics; Volume of fluid; Herschel-Bulkley model

1. Introduction

The construction of offshore infrastructure brings great challenges to the engineers due to the very completed geologic engineering environment in oceans. Specifically, the challenging problem, about the security of pipelines and platforms under the impact of submarine debris flow, are all responsible for the major advances in the understanding of the phenomena of submarine debris flows and their inherent consequences. Submarine debris flow is a kind of catastrophic hazard. That pose great risk to the security and structural integrity of submarine structures such as pipelines and platforms. These events are associated with mass movements that can have a run-out distance of more than 100 km (Locat and Lee, 2002) with a wide coverage area. Subaqueous debris flow is known to travel long distances due to hydroplaning (Mohrig et al., 1998; Piper, 1999) and substantial damages to foundational facilities such as underwater pipelines or cables. An appropriate evaluation of submarine debris flow movements is a major challenge for risk assessment (Locat and Lee, 2002).

Many submarine debris flows are triggered by earthquakes, overloading or are dislodged from steep slopes. (Roberts and Cramp, 1996). Two distinct phenomena can be observed in submarine debris flows: hydroplaning and turbidity currents. Hydroplaning is a thin layer of entrained water at the bottom of the debris flow head which develops due to the influence of bottom friction (Mohrig, 1998) and which usually leads to longer deposition distances (Locat

* Corresponding author e-mail address: yifeicui@ust.hk; liudingzhu@imde.ac.cn;

and Lee, 2002). Turbidity currents are smoke-like sediments dissociated from the debris flow head (Mohrig et al., 2003; Sahaheldin et al., 2000). These phenomena can be observed in both high and low coherent debris flows (Marr 2001). Due to their effects on the flow dynamics and deposition of submarine debris flows, it is important to understand the formation mechanisms of hydroplaning and turbidity current, (Locat and Lee, 2002). The potential damage brought about by these flow events can be calculated by formulas that are functions of the flow velocity, slurry's height, rheology and flow distance (Zakeri, 2009; Haza et al., 2015; Wang, 2016). Iverson (1997) compared flow distance and longitudinal height which are related to the gravitational potential energy and frictional dissipation energy respectively. Results show that the runout distance is highly influenced by different clay and water content. However, these tests were not carried out in a submerged condition. Nonetheless, it could be comprehended that viscosity also influences the energy dissipation process in submarine conditions as well.

Zhu et al. (2013) used two-dimensional (2D) Finite Element Method (FEM) with adaptive mesh technique to simulate large flow deformations and its impact force on submarine pipeline. Results show there is a critical pipe depth at which the where generated drag force is minimum. However, the method is only effective in analysis of specific conditions, and cannot account for hydroplaning, the velocity field that develops, and the turbidity current. Depth Integral Method (DIM) was adopted to simulate landslide flows into the lake (Imran et al., 2001; Marr et al., 2002; Blasio et al., 2004; Sue et al., 2011; Liu et al., 2016). Imran et al. (2001) used a one-dimensional (1D) numerical model to analyze the influence using of different rheological models. Blasio et al. (2004) adopted a 2D numerical model to analyze the mechanisms of hydroplaning. Sue et al. (2011) used this method to analyze tsunamis generated by submarine landslides. Liu et al. (2016) found that bed erosion enhances the damage caused by landslides and increase the possibility of blocking rivers. Pore water pressure has also been found to influences the erosion process.

The algorithms presented are usually two-layer models which assume the interaction between landslides and the ambient water does not involve mass exchange and diffusion. Besides, slurry's morphology and velocity regime cannot be calculated. Smoothed particle hydrodynamics (SPH) coupled with DIM was adopted by Pastor et al. (2009a, 2009b) and Wang et al. (2016) to simulate submarine debris flow. Wang found water depth does not influence flow distance and flow velocity, whereas the friction coefficient and slope influences the maximum velocity and flow distance. This model still cannot calculate the mass diffusion process and hydroplaning's influence was ignored. Gauer et al. (2006) and Zakeri et al. (2009) simulated submarine debris flow movement using Computational Fluid Dynamics (CFD) based on Eulerian-Eulerian multiphase flow theory. Hydroplaning phenomenon was observed although the effects of viscosity were not considered using in detail. Zakeri et al. (2009) used multiple incompressible fluid models in CFX program to analyze the drag force that submarine pipes experience as generated by submarine debris flows. The test conducted a comparison between experimental tests and numerical tests verifying the applicability of a proposed non-Newtonian Reynold's number. Many rheological models were adopted to simulate the rheological characteristics of submarine debris flow: Bingham model (Marr et al., 2002; Pastor et al., 2004; Gauer et al., 2006), Bilinear rheological model (Imran et al., 2001), Power law model (Zakeri et al., 2008) and Herschel-Bulkley model (Imran et al., 2001; Haza et al., 2015). In general, the Herschel-Bulkley model is more adaptive in CFD simulation for the accurate prediction of shear force by instance changing of shear rate (Blasio et al., 2004).

In this study, small-scale tests are carried out using a 3-dimensional (3D) biphasic CFD numerical model. The numerical results bear insight on how viscosity is manifested through the debris flow deposition process.

2. Methodology

2.1. Theory and governing equations

In the current study, the motion of submarine debris material of submarine motion and surrounding water are schematized as two different type of liquid. The Volume of Fluid (VOF) model (Hirt and Nichols, 1981) has been designed for modelling two immiscible fluids phase. The mass continuity of Navier-Stokes equations of submarine flow is shown in Equation 2. Meanwhile, from momentum conservation, the Navier-Stokes equations is expressed in Equation 3, which is a single momentum equation solved throughout the domain, and the resulting velocity field is shared among the phases. Equation 3 is dependent on the volume fractions of all phases through the properties ρ and μ that are calculated from Equation 1.

$$\tilde{\rho} = \sum_{i=1}^3 \alpha_i \rho_i; \tilde{\mu} = \sum_{i=1}^3 \alpha_i \mu_i; \tilde{P} = \sum_{i=1}^3 \alpha_i P_i; \quad (1)$$

$$\tilde{\rho}_i + \nabla(\rho V) = 0 \tag{2}$$

$$(\tilde{\rho V})_i + \vec{V} \cdot \nabla(\tilde{\rho V}) = -\nabla P + \nabla \cdot [\mu(\nabla \vec{V} + \nabla \vec{V}^T)] + \tilde{\rho g} \tag{3}$$

where i states the i th phases of fluid during the calculation, ρ_i is the density of the i th phase; α_i is the volume fraction of i th phase, μ_i is the i th phase dynamic viscosity, P_i is i th fluid pressure; ∇ is the differential operator given in Cartesian coordinates system; \vec{g} is gravity acceleration; \vec{V} is velocity field.

2.2. Calibration and input parameters

The composition of different percent of kaolin clay and Toyoura sand were adopted in this study. Many composition ratio were adopted, but for the flowability under water, three reliable content were adopted. Three tests were conducted, all of which had water and total mass (sum of the mass of kaolin and sand) contents of 50%. sand mass content is 37.5%, 25% and 12.5% in different experiment. After thoroughly mixing, three different slurries with different densities (as shown in Table1) were produced. The rheological respective characteristics were measured using an (Anton Paar Physica MCR301) rheometer. The measured shear stress-strain rate behaviours of the three different samples are shown in Figure 1. Both non-linear rheological models, Power Law, and Herschel-Buckley Model are used to fit the experimental data. The most obvious difference is Power Law Model without yield stress, which influences mechanics during deposition. The Power Law Model and Herschel-Bulkley Model are expressed in Equation 4 and 5, respectively. According to comparison results, Herschel-Bulkley model is more reliable compared with Power Law, and yield stress should be considered.

$$\tau = K\dot{\gamma}^n \tag{4}$$

$$\tau = \tau_c + K\dot{\gamma}^n \tag{5}$$

where τ is shear stress; τ_c is critical shear stress; $\dot{\gamma}$ is shear rate; K and n are adjustment coefficients according to fitted data. The fitting results is shown in Table 2. It is found that all the fitting coefficient is larger than 0.99 for Herschel-Buckley Model, which validate the selection. According to comparison results, the Herschel-Bulkley model best represents the materials' rheology

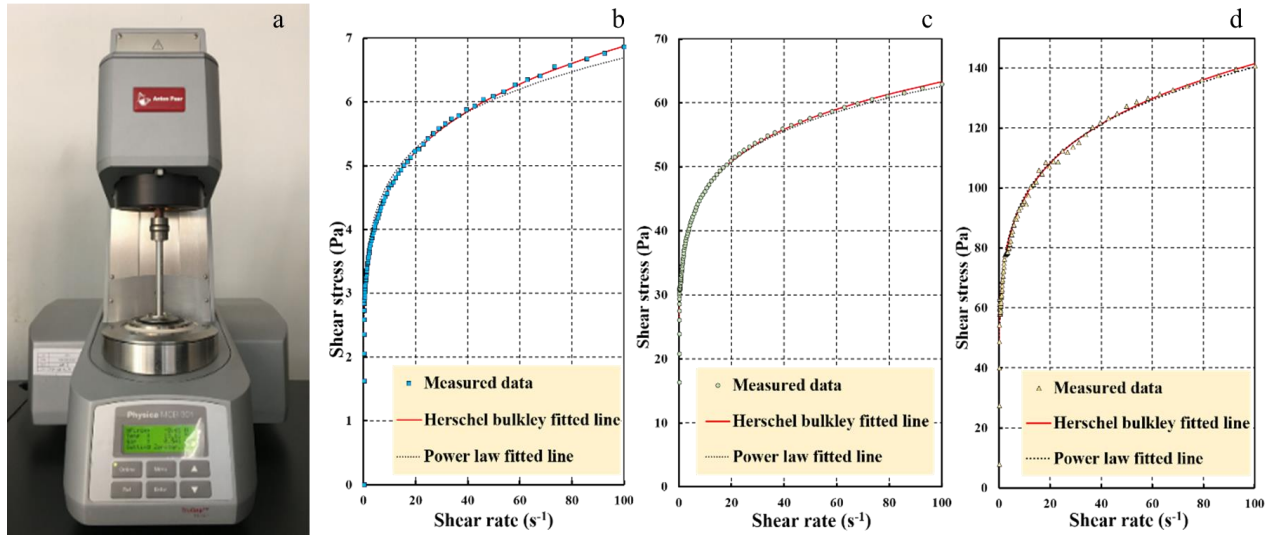


Fig. 1. (a) Rheometer (Anton Paar Physica MCR301); (b) rheological data fitting of RD = 1.406; (c) rheological data fitting of RD = 1.419; (d) rheological data fitting of RD = 1.431; RD means relative density.

Table 1. Rheological fitting (RD means relative density)

| Test ID | Density (kg/m ³) | R ² of Herschel Bulkley model (%) | R ² of Power Law model (%) |
|------------|------------------------------|--|---------------------------------------|
| RD = 1.406 | 1406 | 99.34 | 98.34 |
| RD = 1.419 | 1419 | 99.13 | 98.66 |
| RD = 1.431 | 1431 | 99.11 | 97.88 |

Table 2. Input data of Herschel Bulkley Model

| Test ID | τ_c | K | n |
|------------|----------|--------|-------|
| RD = 1.406 | 1.501 | 1.863 | 0.231 |
| RD = 1.419 | 5.031 | 29.303 | 0.149 |
| RD = 1.431 | 9.307 | 57.803 | 0.179 |

2.3. Domain and boundary conditions

The model was built and meshed in the Gambit 2.4.6b and then transferred into Ansys before the start of calculation. The volume of the storage (0.009 m³) and debris transportation channel is much smaller compared to the water tank (0.6m³). In order to increase the calculation accuracy, the mesh size in the slurry domain (Fig.2 domain a-b-c-d) was set to be as 0.001 m, 0.002 m in the transportation channel (Fig.2 domain b-d-f-e) 0.002 m in the storage (Fig.2 domain g-a-b-h). The mesh size of other remaining domains are 0.020 m. The side view of the model is shown in Figure 2. A total of 1.33 Million meshes were generated in high quality with a value of 0.946 as reported in Ansys Fluent (quality number close to 1 correspond to high quality, the range is between 0 and 1). The boundary condition between water and the wall interface is set as non-slip. This mean that fluid has zero velocity relative to the boundary, consistent to what is observed in experiments (Gue, 2012; Elverhoi et al., 2010).

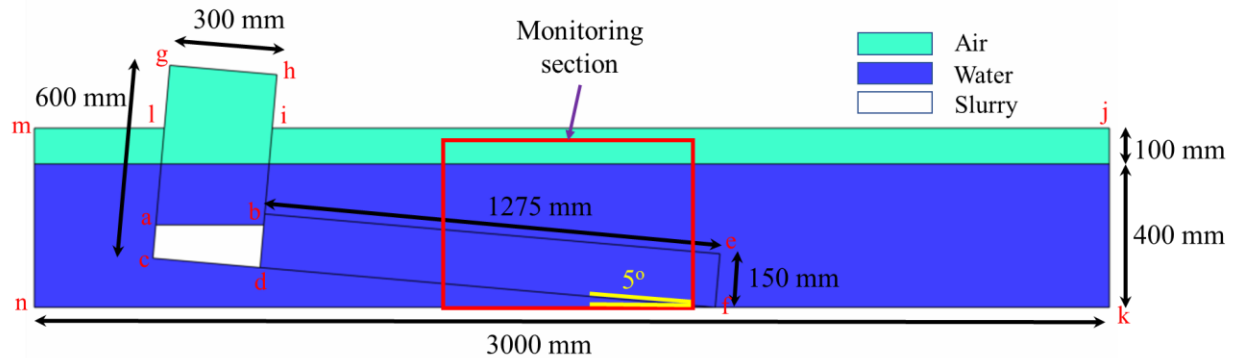


Fig.2. Side view of the 3D Numerical model setup

2.4. Numerical simulation program

Three series of numerical simulations were carried out using different rheological parameters, which were listed in Table 2. The debris slurry is assumed as an incompressible flow. A Pressure-based solver of pressure-velocity coupling algorithm is used to solve the coupled formula of the VOF model. Semi-Implicit Method for Pressure-Linked Equations-Consistent (SIMPLEC) algorithm was adopted to solve this problem with the aims of achieving relative quick convergence. The time step was set as 0.001s determined using von Neumann stability method (Anderson and Wendt, 1995). Maximum iterations were set as 30 steps for calculation convergence and autosave per 100 steps. The acceleration due to gravity is 9.81 m/s² in all the tests. This model includes three phases: air, water, and slurry. Air and water properties are shown in Table.3.

Table 3. Physical character of air and water phase

| Fluid Phase | Density (kg/m^3) | Viscosity ($\text{kg}/(\text{m} \cdot \text{s})$) |
|-------------|------------------------------------|---|
| Air | 1.225 | 1.003×10^{-3} |
| Water | 988.2 | 1.789×10^{-5} |

3. Interpretation of results

Figure 3 (a) shows the deposition process of submarine debris flow with $RD = 1.419$. as can be seen, it reflects the deposition process of submarine debris flow. During deposition, as the slurry mixes with the surrounding water, its average water decrease. The mixing process is dominated by the shear stress in the interface of slurry and water. In the head of debris flow, instability between slurry and water would generate a vortex, one part of vortex is in mixed slurry and another part is in pure water area (Fig.3 (b)). The vortex would separate the debris flow into two parts: the tail part which develops like a triangle and a front part which is like a quadrilateral during deposition. In the vertical direction of frontal head, velocity in the middle part of slurry is larger than the bottom part and interface, where the shear stress is higher. The higher velocity area would absorb water into the slurry's head as shown in Fig.3 (b) which promotes the decreasing of density. Apart from this, higher velocity in the middle layer generate hydroplaning in the front most point at which slurry is lifted by the surrounding water (Fig.3). Furthermore, the velocity difference in the vertical direction elongates and deepen the front head.

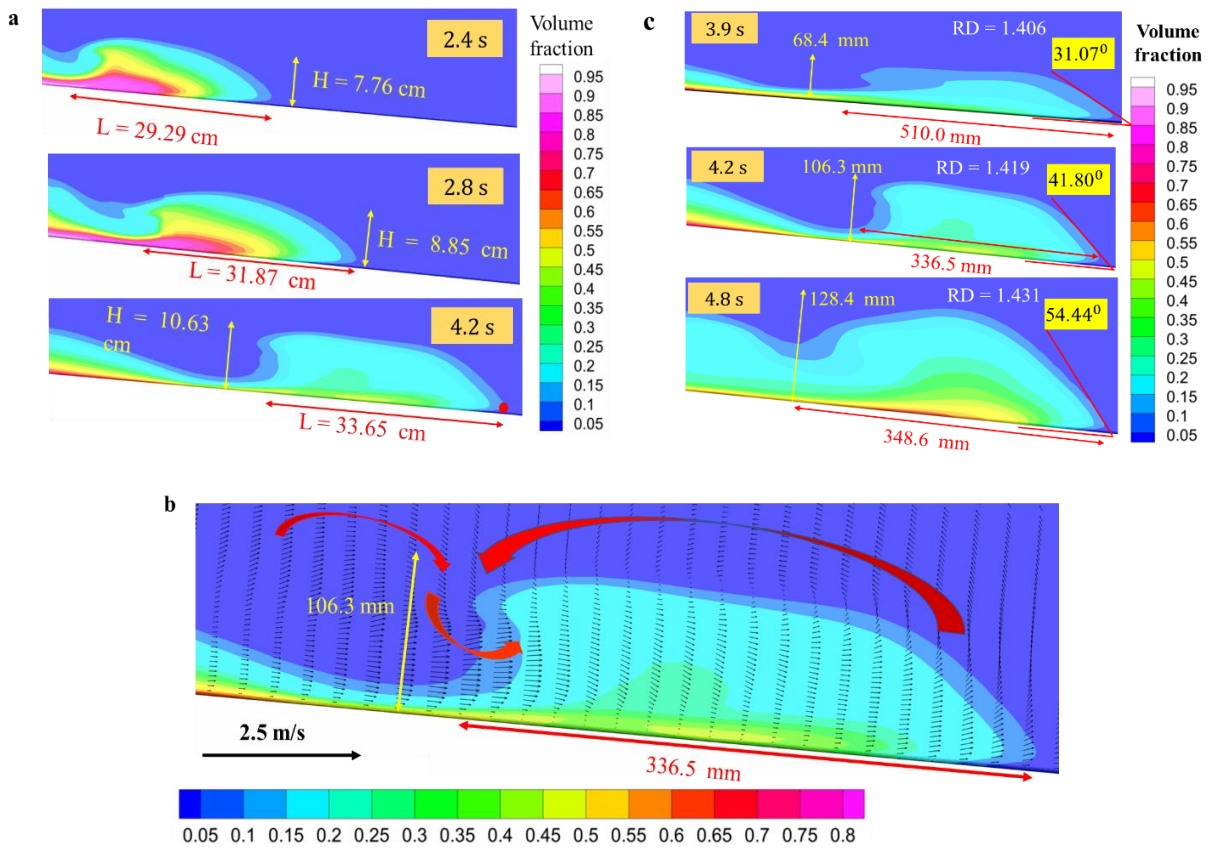


Fig.3. shows the mixing that happens during submarine debris flow deposition (a) the mixture at different times of test for a relative density = 1.419; (b) Flow regime of relative density = 1.419 at 4.2 s; (c) Flow profiles that slurries flow to the end of the channel for different densities.

Denser slurries flow slower than low-density slurries., The time that slurry reach the tail of the channel from the gate opening are 3.9 s, 4.2 s, and 4.8 s respectively. Figure 3 (c) shows the density profile at the time the front head reaches channel's end. High-density slurry flows are thicker both at the front part and at the tail due to high coherency

and viscosity. Higher yield stresses and viscosities generally lead to thicker slurries which can retain their thicknesses. Higher viscosities are related to higher shear stresses at the bottom, interface, and body. This is the reason why the case shows lower fluidity and thicker flow profile. This also leads to a sharper angle at the front head and tail part as well. Sharper angles correspond to lower velocity differences at the vertical section. The ratio of the middle layer's velocity over the distance of the middle layer to bottom is lower than high density case.

For higher density condition, slurry expanded into larger domain, density decreasing process were considered, the averaged density of slurry was calculated from Equation 6, the calculate domain is the mesh that volume fraction of slurry more than 0. The average density is calculated as:

$$\rho(t) = \frac{\sum_{i=1}^N (\alpha_{si} V_i \rho_s + \alpha_{wi} V_i \rho_w)}{\sum_{i=1}^N V_i} \quad (6)$$

where α_{si} is the volume fraction of slurry in mesh i ; α_{wi} is the volume fraction of water in mesh i ; ρ_s is density of slurry; ρ_w is density of water; V_i is volume of mesh i ; the mesh i is a mesh that volume fraction higher than 0.

Figure 4 shows that the averaged density of the slurry decreasing during deposition. This decrease involves two stages. In the first stage (before 2.4 s), the decreasing ratio for each test is higher than the second stage (after 2.4 s). During deposition process, the density decrease ratio (calculated as from Equation 7) of the high-density condition drops quicker than lower-density condition. Compared with the low-density slurry, the decreasing ratio of the high-density slurry is higher in the first stage and lower in the second stage. All these data are concluded in Table.4. The decrease in the density is related to the domain expansion of the slurry which is influenced by the mixtures' rheological characteristics. In the first stage, high viscosity is related to higher shear stress which leads to thicker flows, which creates a larger vortex which results to a higher and larger mixture domain. From these results, high-density slurries expand quicker than low-density slurries. As shown in figure 3 (c), the size of the slurry of the high-density condition is bigger than the low density case. In the second stage, the value of density decreasing ratio is very close, which consequently related to a low decreasing ratio. According to the different expanding ratios, the slurry expands in a relatively manner, which then becomes a stable mass diffusion at the second stage that the slurry. This stage would continue till the end of deposition. The violent expansion at the first stage only lasts for a short time, but it is very important in deposition process.

$$\text{decreasing ratio} = \frac{\text{initial density of this stage} - \text{ending density of this stage}}{\text{slurry density}} \quad (7)$$

where slurry density is the density of slurry before deposition; initial density of this stage means the value of the beginning of this stage; ending density of this stage means the density of the end of this stage.

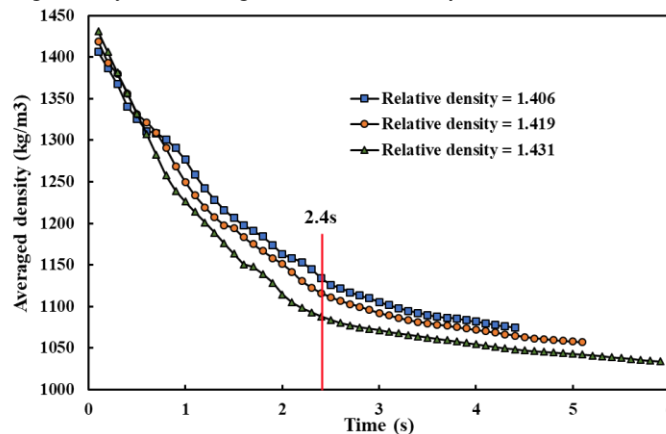


Fig.4. Averaged density decreases during deposition

Table 4. Averaged density decreasing ratio of each test in every stage

| Test ID | Decreasing ratio in stage 1 | Decreasing ratio in stage 2 |
|------------|-----------------------------|-----------------------------|
| RD = 1.406 | 19.33 | 4.21 |
| RD = 1.419 | 21.35 | 4.16 |
| RD = 1.431 | 23.97 | 3.78 |

4. Conclusion

In this study, three numerical analyze were carried out to study the deposition mechanism of submarine debris flows. The deposition process is a process of mass diffusion. In the head of debris flow, shear stress in the interface of slurry and water would generate a huge vortex that separate the debris flow into two parts. This vortex also promotes mass diffusion of the debris flows. High density slurries have higher viscosities, yield shear stresses, and coherency which leads to sharper heads, thicker depths, and larger vortices which are generated by higher shear stress at the interface. The higher velocity layer in the middle part of the slurry enhances the hydroplaning which in turn increase the fluidity of the slurry. Averaged density decrease includes two stages. Density decreases quickly in the first stage in which mass strongly diffuses. In contrast, density decreases slower in the second stage. The quick expansion of deposition happened in short period and stable expansion would last for a long time until the end of deposition.

5. Acknowledgments

The authors would like to thank the National Natural Science Foundation of China (5170091039), the Hong Kong Research Grants Council (IGN15EG03), and the Key Research Program of Frontier Sciences, CAS (No. QYZDY-SSW-DQC006) for their generous support. The authors would also like to thank the theme-based research grant T22-603/15N and general research fund 16209717 of the Hong Kong Research Grants Council. The authors are grateful for financial sponsorship from the Opening Fund of State Key Laboratory of Hydraulics and Mountain River Engineering (SKHL1609) and the support of the HKUST Jockey Club Institute for Advanced Study.

References

- Anderson, J. D., & Wendt, J., 1995, Computational fluid dynamics: New York: McGraw-Hill. ANSYS Inc. ANSYS Fluent, v.206, p. 1-3.
- De Blasio, F. V., Engvik, L., Harbitz, C. B., & Elverhøi, A., 2004, Hydroplaning and submarine debris flows: *Journal of Geophysical Research: Oceans*, 109(C1), doi:10.1029/2002JC001714.
- Elverhoi, A., Breien, H., De Blasio, F. V., Harbitz, C. B., & Pagliardi, M., 2010, Submarine landslides and the importance of the initial sediment composition for run-out length and final deposit. *Ocean Dynamics*, v.60, no. 4, p. 1027-1046, doi: 10.1007/s10236-010-0317-z.
- Gauer, P., Elverhoi, A., Issler, D., & De Blasio, F. V., 2006, On numerical simulations of subaqueous slides: back-calculations of laboratory experiments of clay-rich slides: *Norsk Geologisk Tidsskrift*, v.86, no.3, p. 295.
- Gue, C. S. (2012). Submarine landslide flows simulation through centrifuge modelling [Ph.D. thesis]: Cambridge, University of Cambridge, 33 p.
- Haza, Z.F., Hamonangan, I.S., 2015, On the Numerical Simulations of Drag Forces Exerted by Subaqueous Mudflow on Pipeline: A Laboratory Experiment Assessment. *Proceeding of the 14th International Conference on QIR*, p.181-185.
- Hirt, C. W., & Nichols, B. D., 1981, Volume of fluid (VOF) method for the dynamics of free boundaries: *Journal of computational physics*, v.39, no.1, p. 201-225.
- Imran, J., Harff, P., Parker, Gary., 2001, A numerical model of submarine debris flow with graphical user interface: *Computer & Geosciences*, 27, p. 717-729, doi:org/10.1016/S0098-3004(00)00124-2.
- Iverson, R. M., 1997, The physics of debris flows: *Reviews of geophysics*, v.35, no.3, p. 245-296, doi: 10.1029/97RG00426.
- Liu, W., & He, S., 2016, A two-layer model for simulating landslide dam over mobile river beds: *Landslides*, v.13, no.3, p. 565-576, doi: 10.1007/s10346-015-0585-2.
- Locat, J., & Lee, H. J., 2002, Submarine landslides: advances and challenges: *Canadian Geotechnical Journal*, v.39, no.1, p. 193-212, doi: 10.1139/T01-089.
- Marr, J. G., Elverhøi, A., Harbitz, C., Imran, J., & Harff, P., 2002, Numerical simulation of mud-rich subaqueous debris flows on the glacially active margins of the Svalbard-Barents Sea: *Marine Geology*, v.188, no.3-4, p. 351-364, doi: 10.1016/S0025-3227(02)00310-9.
- Mohrig, D., & Marr, J. G., 2003, Constraining the efficiency of turbidity current generation from submarine debris flows and slides using laboratory experiments. *Marine and Petroleum Geology*, v.20, no.6-8, p. 883-899, doi:10.1016/j.marpetgeo.2003.03.002.
- Mohrig, D., Ellis, C., Parker, G., Whipple, K. X., & Hondzo, M., 1998, Hydroplaning of subaqueous debris flows: *Geological Society of America Bulletin*, v.110, no.3, p. 387-394, doi: 10.1130/0016-7606(1998)110<0387:HOSDF>2.3.CO;2.
- Pastor, M., Quecedo, M., González, E., Herreros, M. I., Merodo, J. F., & Mira, P., 2004, Simple approximation to bottom friction for Bingham fluid depth integrated models: *Journal of Hydraulic Engineering*, v.130, no.2, p. 149-155, doi: 10.1061/(ASCE)0733-9429(2004)130:2(149).

- Pastor, M., Blanc, T., & Pastor, M. J., 2009, A depth-integrated viscoplastic model for dilatant saturated cohesive-frictional fluidized mixtures: application to fast catastrophic landslides: *Journal of Non-Newtonian Fluid Mechanics*, v.158, no.1-3, p. 142-153, doi: 10.1016/j.jnnfm.2008.07.014.
- Pastor, M., Haddad, B., Sorbino, G., Cuomo, S., & Drempetic, V., 2009, A depth-integrated, coupled SPH model for flow-like landslides and related phenomena: *International Journal for numerical and analytical methods in geomechanics*, v.33, no.2, p. 143-172, doi: 10.1002/nag.705.
- Piper, D. J., Cochonat, P., & Morrison, M. L., 1999, The sequence of events around the epicentre of the 1929 Grand Banks earthquake: initiation of debris flows and turbidity current inferred from sidescan sonar: *Sedimentology*, v.46, no.1, p. 79-97, doi: 10.1046/j.1365-3091.1999.00204.x.
- Roberts, J. A., & Cramp, A., 1996, Sediment stability on the western flanks of the Canary Islands: *Marine Geology*, v.134, no.1-2, p. 13-30, doi: 10.1016/0025-3227(96)00021-7.
- Salaheldin, T. M., Imran, J., Chaudhry, M. H., & Reed, C., 2000, Role of fine-grained sediment in turbidity current flow dynamics and resulting deposits: *Marine Geology*, v.171, no.1-4, p. 21-38, doi: 10.1016/S0025-3227(00)00114-6.
- Sue, L. P., Nokes, R. I., & Davidson, M. J., 2011, Tsunami generation by submarine landslides: comparison of physical and numerical models: *Environmental fluid mechanics*, v.11, no.2, p. 133-165, doi: 10.1007/s10652-010-9205-9.
- Wang, Z., Li, X., Liu, P., & Tao, Y., 2016, Numerical analysis of submarine landslides using a smoothed particle hydrodynamics depth integral model: *Acta Oceanologica Sinica*, v.35, no.5, p. 134-140, doi: 10.1007/s13131-016-0864-3.
- Zakeri, A., Høeg, K., & Nadim, F., 2009, Submarine debris flow impact on pipelines—Part II: Numerical analysis: *Coastal engineering*, v.56, no.1, p. 1-10, doi:10.1016/j.coastaleng.2008.06.005.
- Zhu, H., Qi, X., Lin, P., & Yang, Y., 2013, Numerical simulation of flow around a submarine pipe with a spoiler and current-induced scour beneath the pipe: *Applied Ocean Research*, 41, p. 87-100, doi: 10.1061/(ASCE)GM.1943-5622.0000054.